actuators

MDPI

Article

Reliable $L_2 - L_\infty$ Control for Discrete-Time Descriptor Systems with Data Dropouts and Actuator Faults

Qian Yang, Xiao-Heng Chang * and Ming-Yang Qiao

School of Artificial Intelligence and Automation, Wuhan University of Science and Technology, Wuhan 430081, China; yangqian2019@wust.edu.cn (Q.Y.); qiaomingyang@wust.edu.cn (M.-Y.Q.)
* Correspondence: changxiaoheng@wust.edu.cn

Abstract

This paper investigates the reliable stabilization and $L_2 - L_\infty$ performance control problem for discrete-time descriptor systems described by Takagi–Sugeno (T-S) fuzzy models under stochastic data dropouts and actuator faults. In view of the practical situation that system states are usually unmeasurable, a novel observer-based proportional–derivative (PD) control strategy is proposed. Different from traditional state feedback, the PD structure effectively alleviates the inherent structural constraints of descriptor systems and relaxes the conditions for system regularity and causality. By constructing a parameter-dependent Lyapunov functional and using the Schur complement lemma, sufficient conditions are derived in the form of linear matrix inequalities (LMIs) to guarantee the stochastic stability of the closed-loop system and the prescribed $L_2 - L_\infty$ performance. The effectiveness and superiority of the proposed methodology are verified through extensive numerical simulations on two practical case studies, namely, a bio-economic system and a DC motor system. In the case of actuator faults and data dropouts the observer achieves accurate state tracking, and the peak value of the system output is strictly constrained. The research results confirm that the method has strong robustness against data dropouts and actuator faults.

Keywords: descriptor T-S fuzzy systems; observer-based control; $L_2 - L_\infty$ performance; data dropouts

1. Introduction

Descriptor systems, also denoted as singular systems or differential-algebraic equations, incorporate both algebraic constraint subsystems and differential dynamic subsystems into a unified modeling framework [1–5]. This intrinsic structural characteristic endows descriptor systems with a unique advantage in capturing multi-time-scale dynamic phenomena and intricate inter-component coupling relationships that cannot be accurately described by conventional state-space models, thus enabling a more faithful representation of complex engineering processes in fields such as power grids, aerospace guidance systems, and industrial chemical processes. However, this enhanced modeling flexibility inevitably gives rise to substantial analytical and design complexities: continuous-time descriptor systems tend to exhibit generalized impulsive dynamics, while their discrete-time counterparts are prone to non-causal behavior when the admissibility criteria (regularity, causality and stability) are violated. To address these fundamental challenges, researchers have devoted persistent efforts to developing robust admissibility theories for descriptor systems, leveraging advanced techniques including matrix decomposition and structural characterization to rigorously guarantee the three core admissibility properties [6–8].

Check for updates

Academic Editor: Zhenghua Chen

Received: 27 February 2026
Revised: 19 April 2026
Accepted: 23 April 2026
Published: 3 May 2026

Copyright: © 2026 by the authors. Licensee MDPI, Basel, Switzerland. This article is an open access article distributed under the terms and conditions of the Creative Commons Attribution (CC BY) license.

Early control design efforts for descriptor systems were predominantly centered on state-feedback architectures, whose primary objective was to simultaneously ensure system stability and admissibility. While these state-feedback-based approaches have exhibited theoretical validity for descriptor system stabilization, they invariably rely on sophisticated matrix manipulations and structural decompositions to suppress impulsive or non-causal dynamics, which not only complicates theoretical analysis but also severely restricts their practical engineering applicability. To overcome the bottleneck of unmeasurable full-state information in practical scenarios, a series of alternative control strategies have been proposed, such as static output feedback control [9,10], observer-based control schemes [11,12], and dynamic output feedback techniques [13,14]. In recent years, PD state feedback control has emerged as a powerful alternative to pure proportional feedback for descriptor systems [15,16]. By incorporating derivative information into the feedback loop, PD control directly modulates the generalized derivative response of descriptor systems, inherently regularizing system dynamics and mitigating impulsive behavior without the need for complex coordinate transformations. Consequently, PD-based control strategies have exhibited improved robustness and enhanced transient performance for descriptor systems in various practical scenarios [17–19].

Although linear theories serve as a fundamental analytical basis for descriptor system analysis and synthesis, practical engineering systems invariably exhibit inherent nonlinearities that cannot be adequately captured by linear models. To bridge this gap between linear analytical tools and nonlinear system dynamics, T-S fuzzy models have been widely recognized as a flexible and effective modeling methodology [20,21]. T-S fuzzy models represent nonlinear systems as a convex combination of local linear subsystems activated by membership functions, which enables rigorous stability and performance evaluation through a structured convex optimization framework that balances modeling adaptability with analytical feasibility, despite the inherent complexities in fuzzy-rule-based construction and controller synthesis [22,23]. To date, T-S fuzzy modeling has become an established paradigm for describing nonlinear dynamic systems, and PD state-feedback control strategies have been further extended to the T-S fuzzy descriptor system framework [24–26], laying a solid foundation for the control of nonlinear descriptor systems.

Furthermore, the rapid development of networked control systems (NCSs) has introduced additional challenges induced by non-ideal communication environments. In NCSs, data dropouts, which are caused by congestion or unreliable links, undermine signal reliability and introduce uncertainty. Performance deteriorates further when dropouts occur simultaneously with actuator degradation, such as wear-induced attenuation or partial channel failure. Data dropouts cause intermittent or missing measurement and control signals, degrading system performance and potentially compromising closed-loop system admissibility [27–32]. The existing literature mainly adopts two modeling paradigms to characterize data dropout behavior and derive probabilistic stability and performance conditions, Bernoulli or Markov processes [33,34] and deterministic or switching-based approaches for applying switched or hybrid system theories [35–37]. Recent fault-tolerant control methods address actuator faults by designing active sub-compensators for lumped nonlinearities [38] or utilizing strict fault bounds integrated with event-triggered mechanisms [39]. However, they often entail overly complex compensators or restrictive bounding assumptions. This paper designs a reliable controller using a simple multiplicative fault model, motivated by prior interconnected research and the need for structural simplicity.

In terms of performance evaluation, most existing studies on descriptor system control have focused on H_∞ performance, which is predicated on the restrictive assumption that both external disturbances and system outputs possess finite energy. However, in numerous real-world engineering applications, external disturbances are typically peak-bounded

rather than energy-limited, and the controlled outputs are required to satisfy strict peak constraints to ensure operational safety and performance. This practical engineering demand renders the $L_2 - L_\infty$ or energy-to-peak performance criterion more suitable for practical control design [40,41]. Moreover, the majority of $L_2 - L_\infty$ control studies rely on the unrealistic assumption that full-state information is available. Consequently, observer-based control strategies become indispensable for reconstructing unmeasurable states using available input and output information.

Motivated by the aforementioned interconnected research, this paper investigates the problem of reliable $L_2 - L_\infty$ control design for discrete-time T-S fuzzy descriptor systems subject to stochastic packet dropouts and actuator faults (Figure 1). The main contributions of this paper are threefold:

1. A unified observer-based PD control framework is developed for discrete-time T-S fuzzy descriptor systems with simultaneous consideration of stochastic data dropouts and actuator faults. This integrated design achieves stochastic stability and $L_2 - L_\infty$ performance constraints within a concise and realizable closed-loop structure, providing a unified solution for observer-based fault-tolerant control of nonlinear descriptor systems in networked environments.
2. Different from the traditional feedback control strategy [3], the proposed method introduces differential feedback into both the observer and the controller, thereby eliminating the structural constraints of the descriptor system. This elimination avoids the verification of regularity and causality and significantly reduces the analysis complexity of control synthesis.
3. Based on a parameter-dependent Lyapunov functional and the Schur complement lemma, convex LMIs are derived for the co-design of observer and controller gains. These numerically tractable conditions provide an effective design procedure for reliable $L_2 - L_\infty$ control of the considered systems.

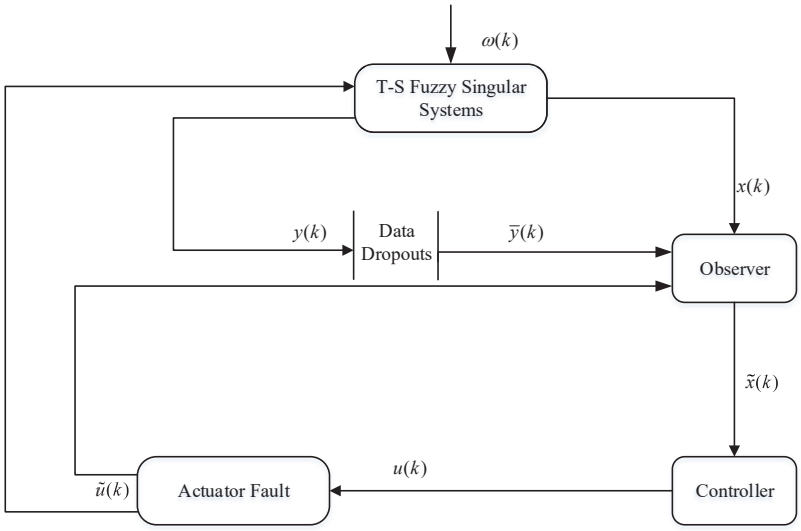


Figure 1. PD control problem of descriptor systems with data dropouts and actuator fault.

The rest of this paper is structured as follows: Section 2 outlines the system formulation, elaborates on the control methodology, and formally defines the problem under investigation. Section 3 derives the LMI-based conditions for stochastic admissibility and $L_2 - L_\infty$ performance, along with the observer and controller synthesis procedure. Section 4, the effectiveness of the proposed method is demonstrated through two cases: the biological economic system and the DC motor driving model. Lastly, Section 5 concludes the paper and outlines potential avenues for future investigation.

Notations. Notations used in this paper are explained as follows. The asterisk $*$ is used to denote a term induced by symmetry. The superscripts "T" and "-1" denote the matrix transposition and matrix inverse, respectively. I and 0 denote the identity matrix and zero matrix with appropriate dimensions, respectively. For a matrix S, $\lambda_{max}(S)$ and $\lambda_{min}(S)$ denote the largest and smallest eigenvalue of S; $He\{S\}$ stands for $S^T + S$. $X \in R^n$ stands for the n-dimensional Euclidean space, whereas $X \in R^{n\times m}$ refers to the whole set of $n \times m$ real matrices. $L_2[0,\infty)$ is the space of square-integrable vector functions over $[0,\infty)$. $\mathbb{E}\{x\}$ and $\mathbb{E}\{x|y\}$ stand for the expectation of the stochastic variable x and the expectation of x conditional on y, respectively. $Pr\{\star\}$ denotes the occurrence probability of the event "$\star$".

2. Problem Formulation and Preliminaries

2.1. T-S Fuzzy System Description

To accurately model the plant's nonlinear dynamics in a unified and analytical manner, we adopt a discrete-time T-S fuzzy model. Under this approach, the overall system is represented as a convex combination of local linear descriptor models, each activated by its corresponding fuzzy membership function.

Plant Rule i: If $\nu_1(k)$ is $\mathcal{G}_{1i}$ and ...$\nu_o(k)$ is $\mathcal{G}_{si}$, then

$$\begin{aligned} Ex(k+1) &= A_i x(k) + B_i \tilde{u}(k) + F_i w(k) \\ y(k) &= C_i x(k) \end{aligned} \tag{1}$$

where $x(k) \in R^{n_x}$ stands for the state vector, $y(k) \in R^{n_y}$ denotes the measured output, and $\tilde{u}(k) \in R^{n_u}$ signifies the applied control input, which accounts for the effects of actuator faults. The external disturbance signal $w(k) \in R^r$ belongs to the space $L_2[0,\infty)$. The matrix E is singular and has rank r with $r < n$, characterizing the singular nature of the system. Matrices A_i, B_i, C_i, and F_i describe the local dynamics of the ith fuzzy rule. The premise variables $\nu_s(k)$ ($s = 1,...,o$) are associated with fuzzy sets $\mathcal{G}_{si}$, where $i = 1,...,v$, and v denote the total number of fuzzy inference rules.

The fuzzy basis function corresponding to Rule i is defined as

$$\varphi_i(\nu(k)) = \frac{\prod_{s=1}^{o} \mathcal{G}_{si}(\nu_s(k))}{\sum_{i=1}^{v}\prod_{s=1}^{o} \mathcal{G}_{si}(\nu_s(k))} \tag{2}$$

where $\mathcal{G}_{si}(\nu_s(k))$ represents the grade of membership function of $\nu_s(k)$ in $\mathcal{G}_{si}$.

The membership functions satisfy the standard convexity properties

$$\varphi_i(\nu(k)) \geq 0, \sum_{i=1}^{v} \varphi_i(\nu(k)) = 1, i = 1,...,v \tag{3}$$

these conditions ensure that the overall T-S fuzzy model represents a convex combination of the local subsystems.

By employing the normalized membership function $\varphi_i(\nu(k))$, the T-S fuzzy model allows the system dynamics to be represented in a compact and efficient form:

$$\begin{aligned} Ex(k+1) &= A(\varphi)x(k) + B(\varphi)\tilde{u}(k) + F(\varphi)w(k) \\ y(k) &= C(\varphi)x(k) \end{aligned} \tag{4}$$

where the system matrices are defined as

$$\begin{aligned} A(\varphi) &= \sum_{i=1}^{v} \varphi_i(\nu(k))A_i, B(\varphi) = \sum_{i=1}^{v} \varphi_i(\nu(k))B_i \\ C(\varphi) &= \sum_{i=1}^{v} \varphi_i(\nu(k))C_i, F(\varphi) = \sum_{i=1}^{v} \varphi_i(\nu(k))F_i \end{aligned} \tag{5}$$

This T-S fuzzy modeling framework provides a systematic bridge between nonlinear system dynamics and linear descriptor subsystems, enabling the application of convex optimization-based analysis and synthesis techniques. In particular, the convex structure induced by the membership functions facilitates stability and performance criteria to be expressed as LMIs, which are amenable to efficient numerical computation.

2.2. Actuator Fault

To account for possible degradation in the actuator channel, an actuator fault model is incorporated into the control input. Specifically, the actual actuator signal is assumed to be a scaled version of the control command generated by the controller, mathematically expressed as

$$\tilde{u}(k) = \eta u(k) \tag{6}$$

where the scalar parameter $\eta \in (0, 1]$ characterizes the level of actuator effectiveness and is assumed to be known. This multiplicative fault model captures a broad class of actuator degradation phenomena commonly encountered in practical systems, such as loss of actuator efficiency, wear-induced attenuation, or partial failure of control channels.

Remark 1. *The proposed actuator fault model encompasses several representative operating scenarios. When $\eta = 1$, the actuator operates under fault-free conditions; in contrast, $\eta \in (0, 1)$ indicates a partial loss of actuator effectiveness, resulting in attenuated control action. The extreme case $\eta = 0$ corresponds to complete actuator failure, in which no control signal is delivered to the plant. This situation is typically addressed through hardware redundancy or fault reconfiguration mechanisms and is therefore excluded from the scope of this study.*

2.3. Data Dropouts

In networked control environments, signal transmission between system components is often subject to data dropouts caused by network congestion, transmission errors, or unreliable communication links. Such data dropouts may occur intermittently and introduce additional uncertainty into the closed-loop system.

To characterize this phenomenon, data dropouts are modeled using a binary stochastic process. Compared with Markovian packet loss models, this approach provides a concise yet effective description of random transmission failures while maintaining analytical tractability. Specifically, the received measurement signal is modeled as

$$\bar{y}(k) = \theta y(k)$$

The random variable θ follows a Bernoulli distribution and takes values exclusively from $(0, 1)$, where

$$\theta = \begin{cases} 0, & \text{packet dropout occurs,} \\ 1, & \text{successful transmission.} \end{cases}$$

The random variable θ is assumed to satisfy:

$$\Pr\{\theta = 1\} = \mathbb{E}\{\theta\} = \bar{\theta}, \quad \Pr\{\theta = 0\} = 1 - \bar{\theta}$$

with $\bar{\theta} \in (0, 1]$ denoting the packet reception probability.

Remark 2. *The Bernoulli-based dropout model captures random and memoryless data dropout behavior, which is suitable for a wide range of communication scenarios. Although more sophisticated models, such as Markov chains, can describe correlated packet losses, the adopted formulation strikes a balance between modeling fidelity and analytical simplicity, facilitating the derivation of tractable stability and performance conditions.*

2.4. PD Observer and Observer-Based PD Controller

To overcome the real-world challenge of inaccessible state variables, a PD observer is developed for state estimation. The observer is constructed to align with the plant's dynamics, ensuring that the convexity characteristics essential for subsequent analysis are maintained.

The PD observer is formulated as

$$\begin{aligned} E\hat{x}(k+1) &= A(\varphi)\hat{x}(k) + B(\varphi)\tilde{u}(k) + L_p(\bar{y}(k) - \bar{\theta}\hat{y}(k)) + L_d(\bar{y}(k+1) - \bar{\theta}\hat{y}(k+1)) \\ \hat{y}(k) &= C(\varphi)\hat{x}(k) \end{aligned} \tag{7}$$

where the estimated state vector is defined as $\hat{x}(k) \in R^{n_x}$ and $\hat{y}(k) \in R^{n_y}$ as estimated output; meanwhile, L_p and L_d stand as the yet-to-be-determined proportional and derivative observer gain matrices.

Based on the estimated state, a PD-type state-feedback controller is designed with an observer structure as follows

$$u(k) = -K_p\hat{x}(k) - K_d\hat{x}(k+1) \tag{8}$$

where K_p and K_d represent the gain matrices of the PD controller, and their appropriate dimensions remain to be determined.

Remark 3. *The incorporation of derivative feedback in both the observer and controller provides an effective mechanism for handling singular dynamics. By directly influencing the generalized difference behavior, PD-based schemes inherently suppress impulsive modes and relax structural constraints associated with descriptor systems, without requiring explicit system decomposition [3,4,15,16]. Following the methodology presented in [42], the present time instant is denoted as $k+1$, whereas the immediately prior time instant is denoted as k. In real-time operation, the state estimate $\hat{x}(k+1)$ needs to be completed within the sampling period.*

2.5. Closed-Loop T-S Fuzzy Descriptor Systems

Let the estimation error of the system state be denoted by

$$e(k) = x(k) - \hat{x}(k) \tag{9}$$

Taking the difference between the plant dynamics and the observer dynamics yields

$$Ee(k+1) = Ex(k+1) - E\hat{x}(k+1) \tag{10}$$

Based on the preceding equation, one can derive the result

$$\begin{aligned} Ex(k+1) &= (A(\varphi) - \eta B(\varphi)K_p)x(k) + \eta B(\varphi)K_p e(k) \\ &\quad - \eta B(\varphi)K_d x(k+1) + \eta B(\varphi)K_d e(k+1) + F(\varphi)w(k) \\ Ee(k+1) &= A(\varphi)e(k) + F(\varphi)w(k) - P_{term} - D_{term} \end{aligned} \tag{11}$$

where the proportional and derivative correction terms induced by packet dropouts are given as follows:
P-term (at time k):

$$\begin{aligned}\text{P-term} &= L_p\left[(\bar{\theta}+\tilde{\theta})C(\varphi)x(k) - \bar{\theta}C(\varphi)\hat{x}(k)\right] \\ &= \bar{\theta}L_pC(\varphi)e(k) + \tilde{\theta}L_pC(\varphi)x(k)\end{aligned}$$

D-term (at time $k+1$):

$$\begin{aligned}\text{D-term} &= L_d\left[(\bar{\theta}+\tilde{\theta})C(\varphi)x(k+1) - \bar{\theta}C(\varphi)\hat{x}(k+1)\right] \\ &= \bar{\theta}L_dC(\varphi)e(k+1) + \tilde{\theta}L_dC(\varphi)x(k+1)\end{aligned}$$

with $\tilde{\theta} = \theta - \bar{\theta}$ denoting the zero-mean stochastic component associated with data dropouts.

To facilitate compact representation and subsequent stability analysis, we define the augmented state vector

$$\xi(k) = \begin{bmatrix} x^T(k) & e^T(k)\end{bmatrix}^T$$

By combining the plant's dynamic behavior with the dynamics governing the estimation error, the closed-loop system can be expressed as a stochastic descriptor system of the form

$$\mathcal{E}_{cl}(\varphi)\xi(k+1) = \mathcal{A}_{cl}(\varphi)\xi(k) + \mathcal{F}_{cl}(\varphi)w(k) \tag{12}$$

where

$$\begin{aligned}\mathcal{E}_{cl}(\varphi) &= \begin{bmatrix} E+\eta B(\varphi)K_d & -\eta B(\varphi)K_d \\ \tilde{\theta}L_dC(\varphi) & E+\bar{\theta}L_dC(\varphi)\end{bmatrix}, \mathcal{F}_{cl}(\varphi) = \begin{bmatrix} F(\varphi) \\ F(\varphi)\end{bmatrix} \\ \mathcal{A}_{cl}(\varphi) &= \begin{bmatrix} A(\varphi)-\eta B(\varphi)K_p & \eta B(\varphi)K_p \\ -\tilde{\theta}L_pC(\varphi) & A(\varphi)-\bar{\theta}L_pC(\varphi)\end{bmatrix}\end{aligned} \tag{13}$$

To facilitate Lyapunov-based stability analysis and $L_2 - L_\infty$ performance synthesis, the stochastic closed-loop system (12) is further decomposed into deterministic and stochastic components. Specifically, we define

$$\tilde{\mathcal{E}} = \bar{\mathcal{E}} + \tilde{\theta}\mathcal{M}_1$$

and we can reinterpret the closed-loop system as

$$\begin{aligned}\tilde{\mathcal{E}}\xi(k+1) &= \left(\bar{\mathcal{A}} + \tilde{\theta}\mathcal{M}_2\right)\xi(k) + \bar{\mathcal{F}}w(k) \\ y(k) &= \bar{\mathcal{C}}\xi(k)\end{aligned} \tag{14}$$

where

$$\begin{aligned}\bar{\mathcal{E}} &= \begin{bmatrix} E+\eta B(\varphi)K_d & -\eta B(\varphi)K_d \\ 0 & E+\bar{\theta}L_dC(\varphi)\end{bmatrix}, \mathcal{M}_1 = \begin{bmatrix} 0 & 0 \\ L_dC(\varphi) & 0\end{bmatrix}, \mathcal{M}_2 = \begin{bmatrix} 0 & 0 \\ -L_pC(\varphi) & 0\end{bmatrix} \\ \bar{\mathcal{A}} &= \begin{bmatrix} A(\varphi)-\eta B(\varphi)K_p & \eta B(\varphi)K_p \\ 0 & A(\varphi)-\bar{\theta}L_pC(\varphi)\end{bmatrix}, \bar{\mathcal{C}} = \begin{bmatrix} C(\varphi) & 0\end{bmatrix}, \bar{\mathcal{F}} = \begin{bmatrix} F(\varphi) \\ F(\varphi)\end{bmatrix}\end{aligned}$$

Definition 1. *The closed-loop system (14) is said to be controllable and observable, if for all $|v| > 1$ and $\forall v \in \mathbb{C}$, the following conditions hold:*

$$rank\begin{bmatrix} vE - A_i \\ C\end{bmatrix} = rank\begin{bmatrix} E \\ C\end{bmatrix} = n_x$$

and

$$rank[\ vE - A_i \ \ B_i\ ] = rank[\ E \ \ B_i\ ] = n_x$$

where n_x denotes the dimensions of the state vector $x(k)$.

Remark 4. *Based on Definition 1, the extended closed-loop system described in (14) fulfills both controllability and observability requirements. Furthermore, the invertibility of $\bar{\mathcal{E}}$ ensures the elimination of impulsive dynamics and non-causal behavior in system (4), thereby guaranteeing its regularity and causality.*

Definition 2. *The closed-loop system (14) is said to be stochastically stable in the mean square if there is a finite $\mathbb{Q} > 0$ for an external disturbance $w(k) = 0$ and initial condition $\xi(0)$, then the following relationship holds*

$$\mathbb{E}\left\{\sum_{k=0}^{\infty} \|\xi(k)\|^2 \,\middle|\, \xi(0)\right\} < \xi^T(0)\mathbb{Q}\xi(0) \tag{15}$$

Then, given a scalar $\gamma > 0$, the PD controller design problem for the discrete-time descriptor system meets the following:
(i) In the absence of $w(k) = 0$, the closed-loop system (14) is stochastically stable.
(ii) Under zero initial conditions, the closed-loop (14) with the designed controller guarantees the prescribed $L_2 - L_\infty$ performance level γ, meaning that for any non-zero $w(k)$, the regulated output $y(k)$ satisfies

$$\mathbb{E}\{\|y(k)\|_\infty\} < \gamma\|w(k)\|_2 \tag{16}$$

with $\|y(k)\|_\infty = sup_{k\in\mathbb{N}}\sqrt{y^T(k)y(k)}$ and $\|w(k)\|_2 = \sum_{k=0}^{\infty}\sqrt{w^T(k)w(k)}$.

3. Main Results

3.1. $L_2 - L_\infty$ Performance Analysis

Theorem 1. *For a prescribed $L_2 - L_\infty$ performance index $\gamma > 0$, the closed-loop system (14) is stochastically stable if there exists a common positive definite matrix $P > 0$, satisfying the following matrix inequalities:*

$$\begin{bmatrix} \delta^2\mathcal{M}_2^T P\mathcal{M}_2 - \bar{\mathcal{E}}^T P\bar{\mathcal{E}} & * & * \\ 0 & -I & * \\ \bar{\mathcal{A}} & \bar{\mathcal{F}} & -P^{-1} \end{bmatrix} < 0 \tag{17}$$

$$\begin{bmatrix} -\gamma^2\bar{\mathcal{E}}^T P\bar{\mathcal{E}} & * \\ \bar{\mathcal{C}} & -I \end{bmatrix} < 0 \tag{18}$$

Proof. The validation process consists of two sequential phases: first, we confirm the stochastic stability of the closed-loop system (14); second, we assess whether the system satisfies the specified $L_2 - L_\infty$ performance requirement.

To analyze the stochastic stability of the closed-loop system, we consider the following Lyapunov functional candidate:

$$V(\xi(k)) = \xi^T(k)\tilde{\mathcal{E}}^T P\tilde{\mathcal{E}}\xi(k),\ \tilde{\mathcal{E}}^T P\tilde{\mathcal{E}} \geq 0.$$

Computing the forward difference of the Lyapunov function evaluated along the solution trajectory of system (14), while incorporating its stochastic characteristics

$$\mathbb{E}\{\tilde{\theta}\} = 0, \mathbb{E}\{\tilde{\theta}^2\} = \bar{\theta}(1 - \bar{\theta}) = \delta^2$$

We derive the following result

$$\begin{aligned}\mathbb{E}\{\Delta V(\xi(k))\} =&\mathbb{E}\{V(\xi(k+1))\} - \mathbb{E}\{V(\xi(k))\}\\ =&\mathbb{E}\{(\bar{\mathcal{A}}+\tilde{\theta}\mathcal{M}_2)\xi(k)+\bar{\mathcal{F}}w(k))^T P(\bar{\mathcal{A}}+\tilde{\theta}\mathcal{M}_2)\xi(k)+\bar{\mathcal{F}}w(k))\}\\ &-\mathbb{E}\{\xi^T(k)\bar{\mathcal{E}}^T P\bar{\mathcal{E}}\xi(k)\}\\ =&\xi^T(k)\bar{\mathcal{A}}^T P\bar{\mathcal{A}}\xi(k)+\xi^T(k)\bar{\mathcal{A}}^T P\bar{\mathcal{F}}w(k)+\delta^2\xi^T(k){\mathcal{M}_2}^T P\mathcal{M}_2\xi(k)\\ &+w^T(k)\bar{\mathcal{F}}P\bar{\mathcal{A}}\xi(k)+w^T(k)\bar{\mathcal{F}}P\bar{\mathcal{F}}w(k)-\xi^T(k)\bar{\mathcal{E}}^T P\bar{\mathcal{E}}\xi(k)\\ &-\delta^2\xi^T(k){\mathcal{M}_1}^T P\mathcal{M}_1\xi(k)\\ \leq&\xi^T(k)\bar{\mathcal{A}}^T P\bar{\mathcal{A}}\xi(k)+\xi^T(k)\bar{\mathcal{A}}^T P\bar{\mathcal{F}}w(k)+\delta^2\xi^T(k){\mathcal{M}_2}^T P\mathcal{M}_2\xi(k)\\ &+w^T(k)\bar{\mathcal{F}}P\bar{\mathcal{A}}\xi(k)+w^T(k)\bar{\mathcal{F}}P\bar{\mathcal{F}}w(k)-\xi^T(k)\bar{\mathcal{E}}^T P\bar{\mathcal{E}}\xi(k)\end{aligned} \tag{19}$$

By using the Schur complement to (17), we can obtain

$$\begin{bmatrix}\delta^2\mathcal{M}_2^T P\mathcal{M}_2-\bar{\mathcal{E}}^T P\bar{\mathcal{E}}+\bar{\mathcal{A}}^T P\bar{\mathcal{A}} & *\\ \bar{\mathcal{F}}^T P\bar{\mathcal{A}} & -I+\bar{\mathcal{F}}^T P\bar{\mathcal{F}}\end{bmatrix}<0$$

and applying the congruence property with $\varrho(k) = col\{\xi(k), w(k)\}$, the result of this analysis is as follows

$$\mathbb{E}\{\Delta V(\xi(k))\} - w^T(k)w(k) < 0 \tag{20}$$

For $w(k) = 0$, we can obtain the following condition from (17),

$$\begin{bmatrix}\delta^2{\mathcal{M}_2}^T P\mathcal{M}_2-\bar{\mathcal{E}}^T P\bar{\mathcal{E}} & *\\ \bar{\mathcal{A}} & -P^{-1}\end{bmatrix}<0 \tag{21}$$

by using Schur complement to (21), we can obtain the equivalent condition:

$$\Pi = \bar{\mathcal{A}}^T P\bar{\mathcal{A}}+\delta^2\mathcal{M}_2^T P\mathcal{M}_2-\bar{\mathcal{E}}^T P\bar{\mathcal{E}}<0$$

since Π is a symmetric negative definite matrix, for any non-zero state vector $\xi(k)$, the quadratic form satisfies:

$$\xi^T(k)(\bar{\mathcal{A}}^T P\bar{\mathcal{A}}+\delta^2\mathcal{M}_2^T P\mathcal{M}_2-\bar{\mathcal{E}}^T P\bar{\mathcal{E}})\xi(k)<0$$

substituting the above solution into the Lyapunov difference $\mathbb{E}\{\Delta V(\xi(k))\}$, we have

$$\begin{aligned}\mathbb{E}\{\Delta V(\xi(k))\} &= \mathbb{E}\{V(\xi(k+1))\} - \mathbb{E}\{V(\xi(k))\}\\ &\leq \xi^T(k)\Pi\xi(k) < 0\end{aligned} \tag{22}$$

Since $\Pi < 0$, the matrix $-\Pi$ is positive definite, and we denote $\lambda_{\min}(-\Pi) > 0$ as the minimum eigenvalue of the matrix $-\Pi$. For any vector $\xi(k)$, the quadratic form satisfies:

$$\xi^T(k)(-\Pi)\xi(k) \geq \lambda_{\min}(-\Pi)\|\xi(k)\|^2$$

and rearranging the above inequality gives:

$$\xi^T(k)\Pi\xi(k) \leq \lambda_{\min}(-\Pi)\|\xi(k)\|^2$$

Substituting back into the Lyapunov difference, we obtain the key equality:

$$\begin{aligned}\mathbb{E}\{\Delta V(\xi(k))\} &= \mathbb{E}\{V(\xi(k+1))\} - \mathbb{E}\{V(\xi(k))\} \\ &= \mathbb{E}\{\xi^T(k+1)\tilde{\mathcal{E}}^T P\tilde{\mathcal{E}}\xi(k+1)\} - \xi^T(k)\tilde{\mathcal{E}}^T P\tilde{\mathcal{E}}\xi(k) \\ &\leq \xi^T(k)\Pi\xi(k) \\ &\leq -\lambda_{\min}(-\Pi)\mathbb{E}\{\|\xi(k)\|^2\}\end{aligned} \tag{23}$$

Computing the unconditional expectation of both sides of the aforementioned equation for any positive integer $l \geq 1$ and then summing the resulting expressions from $k = 0, ..., l$, we obtain

$$\begin{aligned}&\mathbb{E}\{\xi^T(k+1)\tilde{\mathcal{E}}^T P\tilde{\mathcal{E}}\xi(k+1)\} - \xi^T(0)\tilde{\mathcal{E}}^T P\tilde{\mathcal{E}}\xi(0) \\ \leq &-\lambda_{\min}(-\Pi)\sum_{k=0}^{l}\mathbb{E}\{\|\xi(k)\|^2\}\end{aligned} \tag{24}$$

which means that

$$\begin{aligned}&\sum_{k=0}^{l}\mathbb{E}\{\|\xi(k)\|^2\} \\ \leq &(\lambda_{\min}(-\Pi))^{-1}(\xi^T(0)\tilde{\mathcal{E}}^T P\tilde{\mathcal{E}}\xi(0) - \mathbb{E}\{\xi^T(l+1)\tilde{\mathcal{E}}^T P\tilde{\mathcal{E}}\xi(l+1)\})\end{aligned} \tag{25}$$

Since the Lyapunov function is defined as $V(\xi(k)) = \xi^T(k)\tilde{\mathcal{E}}^T P\tilde{\mathcal{E}}\xi(k)$, for any state, we have $\mathbb{E}\{\xi^T(l+1)\tilde{\mathcal{E}}^T P\tilde{\mathcal{E}}\xi(l+1))\} \geq 0$ for any $l \geq 1$. At this juncture, the inequality (24) becomes:

$$\mathbb{E}\{\sum_{k=0}^{\infty}\|\xi(k)\|^2 \,|\, \xi(0)\} \leq (\lambda_{\min}(-\Pi))^{-1}\xi^T(0)\lambda_{\max}(\tilde{\mathcal{E}}^T P\tilde{\mathcal{E}})\xi(0) \tag{26}$$

$$= \xi^T(0)\underbrace{(\lambda_{\min}(-\Pi))^{-1}\lambda_{\max}(\tilde{\mathcal{E}}^T P\tilde{\mathcal{E}})}_{\mathbb{Q}}\xi(0) \tag{27}$$

where $\xi(0)$ is the initial condition, and $\mathbb{Q} = (\lambda_{\min}(-\Pi))^{-1}\lambda_{\max}(\tilde{\mathcal{E}}^T P\tilde{\mathcal{E}})$. Then, it can be obtained that the close-loop system is stochastically stable with Definition 2 if condition (17) is given.

Next, the $L_2 - L_\infty$ performance of the closed-loop system (14) is investigated under zero initial conditions and $w(k) \neq 0$. In this case, inequality (20) reduces to

$$\mathbb{E}\{\Delta V(\xi(k))\} < w^T(k)w(k) \tag{28}$$

Adding up the inequality over the range from 0 to $k-1$ yields

$$\begin{aligned}\sum_{\ell=0}^{k-1}\mathbb{E}\{\Delta V(\xi(\ell))\} &= \mathbb{E}\{V(\xi(k))\} \\ &< \sum_{\ell=0}^{k-1} w^T(\ell)w(\ell)\end{aligned} \tag{29}$$

We further obtain

$$\mathbb{E}\{V(\xi(k))\} + w^T(k)w(k) < \sum_{\ell=0}^{k} w^T(\ell)w(\ell) \tag{30}$$

Meanwhile, using the Schur complement to (18) and combining it with the state vector $\xi(k)$, then taking the quadratic form of it, we can obtain

$$\begin{aligned}\mathbb{E}\{y^T(k)y(k)\} &< \gamma^2\mathbb{E}\{V(\xi(k)) + w^T(k)w(k)\} \\ &< \gamma^2\sum_{\ell=0}^{k} w^T(\ell)w(\ell)\end{aligned} \tag{31}$$

Finally, taking the supremum of $y^T(k)y(k)$ over time k, it is natural to get the following condition

$$\|y(k)\|_\infty < \gamma\|w(k)\|_2 \tag{32}$$

This result shows that the closed-loop system (14) satisfies the $L_2 - L_\infty$ performance criterion specified in Definition 2. The proof process has been successfully concluded. □

The foregoing analysis rigorously establishes both stochastic stability and $L_2 - L_\infty$ performance for the closed-loop system under the proposed PD control strategy. However, the design conditions in Theorem 1 are not directly tractable. To tackle this challenge, we employ a scaling inequality technique, transforming the original conditions into LMIs. These LMIs then serve as the foundation for establishing practical design conditions for both the observer-based PD controller and the PD observer.

3.2. Observer-Based PD State Feedback Controller Design

Theorem 1 establishes a solid theoretical foundation for analyzing the $L_2 - L_\infty$ performance of system (14). Leveraging this result, we develop a PD-type state-feedback controller that incorporates an observer. To ensure tractability in the design process, we formulate a set of convex LMIs that simultaneously determine the observer gains L_p, L_d and the controller gains K_p, K_d. The resulting closed-loop system (14) is guaranteed to be stochastically stable, while its $L_2 - L_\infty$ gain is ensured to remain below the prescribed level γ.

Theorem 2. *Consider the closed-loop system described in (14). For given scalars $\gamma > 0$ and $\bar{\theta}$, if there exist positive definite matrices $Q_1 > 0$, $Q_3 > 0$, a symmetric Q_2, and gain matrices K_p, K_d, L_p, and L_d of appropriate dimensions such that the following LMIs hold:*

$$\Pi_1^i < 0, i = 1, ..., v \tag{33}$$

$$\Pi_2^i < 0, i = 1, ..., v \tag{34}$$

where

$$\Pi_1^i = \begin{bmatrix} \Theta_1 & * & * & * \\ 0 & -I & * & * \\ \Theta_{21} & \Theta_{22} & -Q & * \\ \Theta_{31} & 0 & 0 & -Q \end{bmatrix}$$

$$\Pi_2^i = \begin{bmatrix} \Theta_4 & * \\ \Theta_5 & -I \end{bmatrix}$$

$$Q = \begin{bmatrix} Q_1 & * \\ Q_2 & Q_3 \end{bmatrix}, \Theta_1 = \begin{bmatrix} -He\{E + \eta B_i K_d\} + Q_1 & * \\ (\eta B_i K_d)^T + Q_2 & -He\{E + \bar{\theta} L_d C_i\} + Q_3 \end{bmatrix}$$

$$\Theta_{21} = \begin{bmatrix} A_i - \eta B_i K_p & \eta B_i K_p \\ 0 & A_i - \bar{\theta} L_p C_i \end{bmatrix}, \Theta_{22} = \begin{bmatrix} F_i \\ F_i \end{bmatrix}, \Theta_{31} = \begin{bmatrix} 0 & 0 \\ \delta L_p C_i & 0 \end{bmatrix}$$

$$\Theta_4 = \begin{bmatrix} -He\{\gamma^2 E + \gamma^2 \eta B_i K_d\} + \gamma^2 Q_1 & * \\ (\gamma^2 \eta B_i K_d)^T + \gamma^2 Q_2 & -He\{\gamma^2 E + \gamma^2 \bar{\theta} L_d C_i\} + \gamma^2 Q_3 \end{bmatrix}$$

$$\Theta_5 = \begin{bmatrix} C_i & 0 \end{bmatrix}$$

then the $L_2 - L_\infty$ performance γ of the closed-loop descriptor system (14) can be guaranteed through the integration of the PD controller (8) and the observer (7).

Proof. The proof is carried out by deriving tractable sufficient conditions for quadratic performance inequality (16) to hold and by reformulating them into a convex LMI framework suitable for controller and observer synthesis. First, by invoking the Schur complement on condition (17), the inequality can be restated as

$$\begin{bmatrix} -\bar{\mathcal{E}}^T P \bar{\mathcal{E}} & * & * & * \\ 0 & -I & * & * \\ \bar{\mathcal{A}} & \bar{\mathcal{F}} & -P^{-1} & * \\ \delta \mathcal{M}_2 & 0 & 0 & -P^{-1} \end{bmatrix} < 0 \tag{35}$$

To linearize this nonlinear term, we introduce the following well-known scaling inequality: for any positive definite matrix $P > 0$ and any compatible matrix G, the inequality $(P - G)^T P^{-1} (P - G) \geq 0$ always holds. From this, it follows that $-G^T P^{-1} G < -G - G^T + P$.

Substituting the above inequality into (35) and (18), the following results can be obtained

$$\begin{bmatrix} -\bar{\mathcal{E}}^T - \bar{\mathcal{E}} + P^{-1} & * & * & * \\ 0 & -I & * & * \\ \bar{\mathcal{A}} & \bar{\mathcal{F}} & -P^{-1} & * \\ \delta \mathcal{M}_2 & 0 & 0 & -P^{-1} \end{bmatrix} < 0 \tag{36}$$

$$\begin{bmatrix} \gamma^2(-\bar{\mathcal{E}}^T - \bar{\mathcal{E}} + P^{-1}) & * \\ \bar{\mathcal{C}} & -I \end{bmatrix} < 0 \tag{37}$$

In order to simultaneously synthesize the observer and PD controller gains, the inverse Lyapunov matrix is parameterized in the following structured form:

$$P^{-1} = Q = \begin{bmatrix} Q_1 & * \\ Q_2 & Q_3 \end{bmatrix}$$

where $Q_1 > 0$ and $Q_3 > 0$ are positive definite matrices. This structured decomposition facilitates the decoupling of decision variables associated with the controller and observer gains.

Subsequently, by applying appropriate variable substitutions and congruence transformations, inequalities (33) and (34) can be equivalently reformulated as LMIs (36) and (37) for all $i = 1, ..., v$. These transformations directly establish the design conditions for the observer-based PD controller. Consequently, the feasibility of LMIs (36) and (37) guarantees that the closed-loop descriptor system (14) is stochastically stable and strictly achieves the prescribed $L_2 - L_\infty$ performance γ. This concludes the proof. □

Remark 5. *According to the design conditions of Theorem 2, the $L_2 - L_\infty$ control problem of the system (14) can be solved. On this basis, the control performance index γ can be optimized by*

$$min\ \bar{\gamma}$$

subject to LMIs (33) and (34) with $\bar{\gamma} = \gamma^2$, so that the corresponding optimization value of $L_2 - L_\infty$ performance is $\gamma_{min} = \sqrt{\bar{\gamma}_{min}}$.

4. Simulation

In this section, two practical applications are employed to demonstrate the effectiveness of the proposed observer-based PD controller design method.

4.1. Bio-Economic System

A bio-economic system [43] was selected as the case study because it captured the typical features of nonlinear descriptor systems, including algebraic constraints, nonlinear dynamics, and practical constraints commonly encountered in networked and economic–ecological applications. Thus, it served as an appropriate benchmark for verifying the effectiveness and robustness of the proposed approach.

$$\begin{aligned} \frac{dx_1(t)}{dt} &= ax_2(t) - bx_1(t) \\ \frac{dx_2(t)}{dt} &= \bar{\delta}x_1(t) - b\bar{\gamma}x_2^2(t) - x_2(t)x_3(t) \\ 0 &= x_3(t)\big(px_2(t) - c\big) - m \end{aligned} \tag{38}$$

where $x_1(t)$ is the population density of immature species, $x_2(t)$ is the population density of mature species, $x_3(t)$ is harvest effort of harvested mature population. At any time, $(t > 0)$, the birth rate of the immature population is proportional to the density of the existing mature individuals, and the proportionality constant is a. The death rate of the immature population and the rate of transformation of the mature population are proportional to the density of existing immature population with proportionality constant b. $\bar{\delta}$ denotes the proportional transforming rate from the immature population to the mature population. The death rate of the mature population is proportional to the square of the mature population's size with proportionality constant $\bar{\gamma}$. All the parameters mentioned above are positive constants. $p > 0$ is the unit price of mature population. $c > 0$ is the fixed cost of harvesting per unit of effort, and m is the economic profit.

To formulate harvesting strategies and maintain the sustainable development of the system, measures must be taken to stabilize the population size of organisms. Let $a = 0.2$, $b = 0.7$, $\bar{\delta} = 0.05$, $\bar{\gamma} = 0.1$, $p = 1$, $c = 30$, $m = 0$ and assume $|x_2(k)| \leq \mu = 5$, where μ is the carrying capacity of the population.

The membership function can be expressed as

$$\varphi_1(x_2(k)) = \frac{1}{2}\left(1 - \frac{x_2(k)}{\mu}\right), \varphi_2(x_2(k)) = \frac{1}{2}\left(1 + \frac{x_2(k)}{\mu}\right)$$

where

$$\varphi_1(x_2(k)) + \varphi_2(x_2(k)) = 1$$

Selecting a sampling period $T_e = 0.4s$ and using the Euler's first-order approximation, the discrete-time T-S fuzzy system was obtained by the following two fuzzy rules:

$$\text{Rule}^1: \quad \text{If } x_2(k) \text{ is } \pm 5, \text{ then} \quad \begin{cases} Ex(k+1) = A_1x(k) + B_1\tilde{u}(k) + F_1w(k), \\ y(k) = C_1x(k) \end{cases}$$

$$\text{Rule}^2: \quad \text{If } x_2(k) \text{ is } 0, \text{ then} \quad \begin{cases} Ex(k+1) = A_2x(k) + B_2\tilde{u}(k) + F_2w(k), \\ y(k) = C_2x(k) \end{cases}$$

where

$$E = \begin{bmatrix} 1 & 0 & 0 \\ 0 & 1 & 0 \\ 0 & 0 & 0 \end{bmatrix}, A_1 = \begin{bmatrix} -0.0480 & 0.0720 & 0.0088 \\ 0.0184 & 0.3824 & 1.8232 \\ 0 & 0 & -259 \end{bmatrix}, A_2 = \begin{bmatrix} -0.0480 & 0.0696 & -0.0088 \\ 0.0176 & 0.0224 & -1.7776 \\ 0 & 0 & -187 \end{bmatrix}$$
$$B_1 = B_2 = \begin{bmatrix} 0 & 0 \\ 0.4 & 0 \\ 0 & -0.4 \end{bmatrix}, C_1 = C_2 = \begin{bmatrix} 1 & 1 & 0 \\ 0 & 0 & 1 \end{bmatrix}, F_1 = F_2 = \begin{bmatrix} 0.0596 \\ -0.0024 \\ -0.3133 \end{bmatrix}$$

The disturbance was presumed to be

$$w(k) = -0.2sin(2k)e^{-0.1k}$$

Setting the initial condition $x(0) = \hat{x}(0) = \begin{bmatrix} 0 & 0 & 0 \end{bmatrix}^T$ and the data dropouts probabilities as $\theta = 0.4$, the actuator fault parameter was chosen as $\eta = 0.5$, and we specified the desired $L_2 - L_\infty$ performance index $\gamma = 2$.

Next, solving the LMIs given in (33) and (34) yielded the gain matrices for both the controller and the observer

$$\begin{aligned} K_p &= \begin{bmatrix} 0.0693 & 0.0121 & 0.0114 \\ 0.0.34 & 0.0014 & 128.0678 \end{bmatrix}, K_d = \begin{bmatrix} 3.8166 & 10.8692 & 0.9126 \\ -0.0441 & 1.1258 & -1.5575 \times 10^3 \end{bmatrix} \\ L_p &= \begin{bmatrix} 8.5248 \times 10^{-5} & 0.0020 & -0.0044 \\ 1.6530 & 1.4326 & -568.1682 \end{bmatrix}^T, L_d = \begin{bmatrix} 813.7166 & 817.1976 & 1.4466 \\ 1.1590 & 0.2787 & 2.1820 \times 10^3 \end{bmatrix}^T \end{aligned} \tag{39}$$

Figures 2–4 show the responses of system states $x_1(k)$, $x_2(k)$ and $x_3(k)$ and their observer estimates under data dropout, actuator faults, and their simultaneous occurrence. It can be seen that the estimated states closely track the actual states and converge well under all conditions, demonstrating the effectiveness and robustness of the proposed observer-based PD control scheme. Figure 5 shows the system outputs and the corresponding observer outputs. The results indicate that the observer can reconstruct the outputs accurately, thus providing reliable information for feedback control. Figure 6 presents the control inputs $u_1(k)$ and $u_2(k)$. It is clear that the control signals remain bounded and smooth throughout the simulation process. Figure 7 verifies the $L_2 - L_\infty$ performance level of the closed-loop system. The results show that the peak output of the system is always effectively constrained within the specified performance index range under external disturbances.

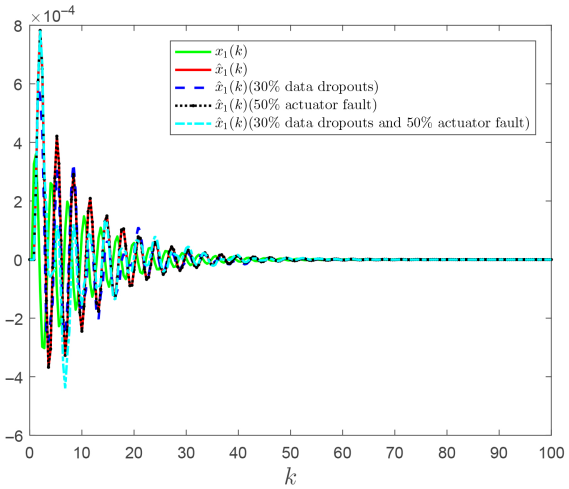


Figure 2. The responses of system state $x_1(k)$ and observer state $\hat{x}_1(k)$ under data dropouts and actuator faults.

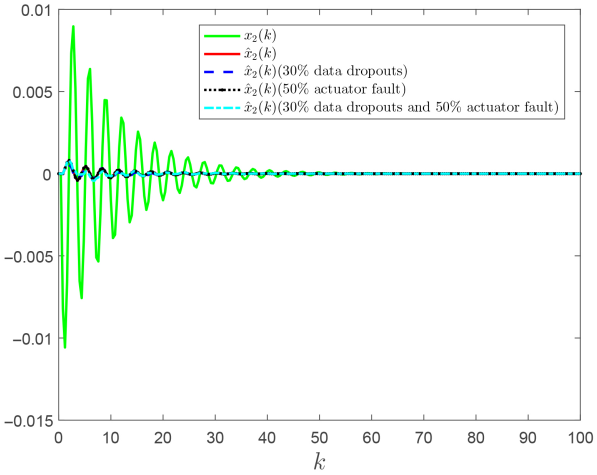


Figure 3. The responses of system state $x_2(k)$ and observer state $\hat{x}_2(k)$ under data dropouts and actuator faults.

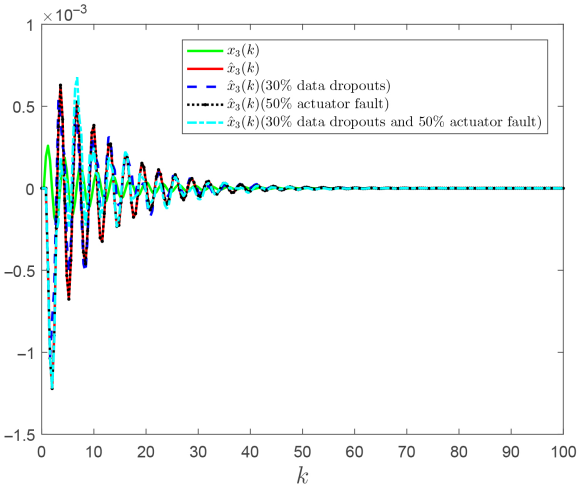


Figure 4. The responses of system state $x_3(k)$ and observer state $\hat{x}_3(k)$ under data dropouts and actuator faults.

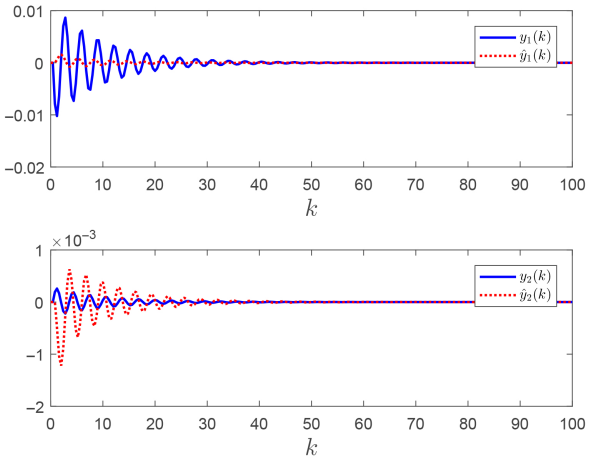


Figure 5. The responses of system output $y_1(k)$ and $y_2(k)$, observer output $\hat{y}_1(k)$ and $\hat{y}_2(k)$.

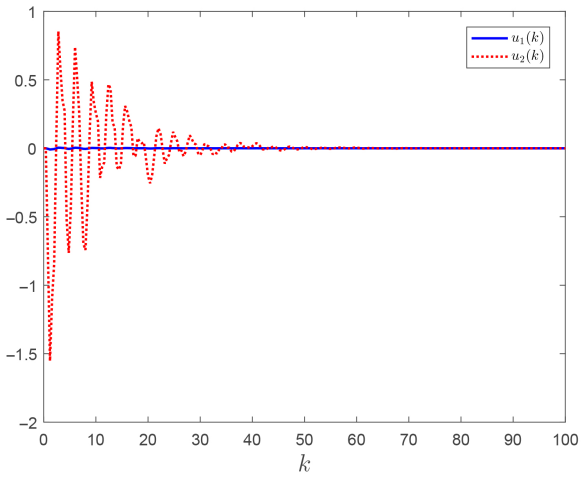


Figure 6. The responses of control input $u_1(k)$ and $u_2(k)$.

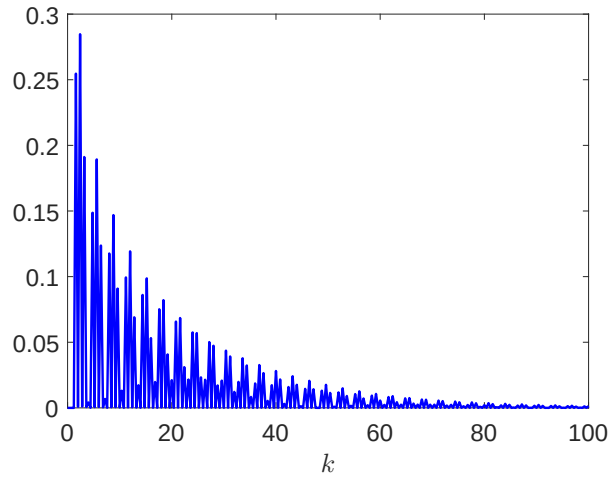


Figure 7. Ratio of $\sqrt{y^T(k)y(k)/\sum_{k=0}^{\infty} w^T(k)w(k)}$.

Furthermore, the performance optimization values in Table 1 were calculated and optimized by adopting the methods in Remark 5; the method of Theorem 2 had a smaller index value compared with [44], indicating that it was less conservative.

Table 1. Minimum $L_2 - L_\infty$ performance index γ_{min}.

Method	**[44]**	**Theorem 2**
γ_{min}	5.3306×10^{-3}	1.1260×10^{-3}

Remark 6. *Actuator fault refers to the efficiency loss of harvesting equipment, which is described by the parameter $\eta = 0.5$. Data dropout refers to the packet loss of population monitoring signals during wireless transmission, with a probability of 30%. Control inputs $u_1(k)$, $u_2(k)$ represent the adjustment of harvesting effort. Disturbance $w(k)$ represents external ecological interference such as climate and natural death rate fluctuations.*

4.2. DC Motor System

In this section, an actual motor model is used to prove the effectiveness of the derived design method. The DC motor-load dynamics model is shown in Figure 8, described by the following mechanical and electrical equations:

$$\begin{cases} J\dot{\omega}(t) = K_t i(t) - b\omega(t) \\ v(t) = R(t)i(t) + K_\omega \omega(t) \end{cases} \tag{40}$$

where $i(t)$ signifies the armature current, $\omega(t)$ is the shaft angular velocity, $v(t)$ is the applied voltage input, and $w(t)$ is the external stochastic load torque disturbance. The constants K_ω and K_t denote the back electromotive force coefficient and torque coefficient, respectively. Moreover, the parameters J and b represent the equivalent moment of inertia and viscous friction coefficient.

For a motor–load system with a gear ratio n, the equivalent inertia and viscous friction forces are given by

$$J = J_m + \frac{J_c}{n^2}, b = b_m + \frac{b_c}{n^2} \tag{41}$$

where J_m and J_c represent the motor and the load inertia values, b_m and b_c denote the corresponding viscous damping coefficients.

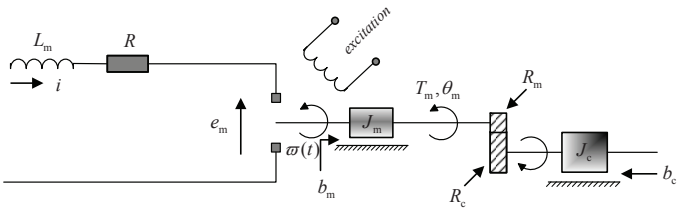


Figure 8. Block diagram of a DC motor.

In practical applications, motor aging and rotor–stator friction lead to nonlinear resistance variations. This phenomenon is modeled as

$$R(t) = R_0 + R_1 i^2(t) \tag{42}$$

where R_0 is the nominal resistance, R_1 is the resistance variation coefficient, and the current range is constrained to $-2 \le i(t) \le 2$, i.e., $0 \le i^2(t) \le 4$.

The parameters of the DC motor-driven mechanical system were selected as: $J_m = 1$ kg, $J_c = 50$ kg, $b_c = 600$, $b_m = 0.1$, $R_0 = 8\ \Omega$, $R_1 = 0.3\ \Omega$, $K_t = 80$ Nm/A, $K_\omega = 2$ Vs/rad, $b_{w1} = 0.6$, $b_{w2} = 0.5$, and $n = 70$.

Let the state vector be defined as $x(t) = \left[x_1^T(t)\ x_2^T(t)\right]^T = [\omega(t)\ i(t)]^T$. Then, set $v(t) = u(t)$ and incorporate the external disturbance denoted as $w(t)$. Substituting the nonlinear resistance into (40), a continuous-time state-space representation of the system is derived

$$\begin{bmatrix} 1 & 0 \\ 0 & 0 \end{bmatrix} \dot{x}(t) = \begin{bmatrix} -\frac{b}{J} & \frac{K_t}{J} \\ K_\omega & R(t) \end{bmatrix} x(t) + \begin{bmatrix} 0 \\ -1 \end{bmatrix} u(t) + \begin{bmatrix} b_{w1} \\ b_{w2} \end{bmatrix} w(t) \tag{43}$$

To approximate the nonlinear system (43), a T-S fuzzy model comprising two rules was employed. This approach represented the nonlinear dynamics as a weighted combination of linear subsystems through the T-S fuzzy framework. The system's T-S fuzzy model was precisely expressed in the following form:

$$E\dot{x}(t) = \sum_{l=1}^{2} \varphi_l(v(t)) \left(A_{la}x(t) + B_{la}\tilde{u}(t) + F_{la}w(t)\right) \tag{44}$$

with $x(t) = \left[x_1^T(t)\ x_2^T(t)\right]^T$, $\varphi_l(v(t))$ as the normalized membership functions.

Defining $v(t) = x_2(t)$, it then becomes evident that the range of $v^2(t)$ is confined within the bounds $0 \leq v^2(t) \leq 4$. Thus, $v^2(t)$ can be expressed as

$$v^2(t) = \varphi_1(v(t)) \times 4 + \varphi_2(v(t)) \times 0, \varphi_1(v(t)) + \varphi_2(v(t)) = 1. \tag{45}$$

Building on the equations discussed above, the membership function can be expressed as

$$\varphi_1(v(t)) = x_2^2(t)/4, \varphi_2(v(t)) = 1 - \varphi_1(v(t))$$

The linear subsystem matrices for the two rules are:

$$A_{1a} = \begin{bmatrix} -0.2202 & 79.1919 \\ 2 & 8 \end{bmatrix}, A_{2a} = \begin{bmatrix} -0.2202 & 79.1919 \\ 2 & 9.2 \end{bmatrix} \tag{46}$$

$$B_{1a} = B_{2a} = \begin{bmatrix} 0 \\ -1 \end{bmatrix}, F_{1a} = F_{2a} = \begin{bmatrix} 0.6 \\ 0.5 \end{bmatrix} \tag{47}$$

The disturbance is presumed to be

$$w(t) = 0.5sin(2t)e^{-0.3t}$$

For digital control implementation, we converted the continuous-time fuzzy model into discrete-time equivalent using Euler's first-order approximation by employing a sampling period $T = 0.1s$. The resulting discrete-time T-S fuzzy descriptor system was characterized by two fuzzy rules:

$$\text{Rule}^1: \quad \text{If } x_2(k) \text{ is } \pm 2, \text{ then}$$
$$\begin{cases} Ex(k+1) = A_1x(k) + B_1\tilde{u}(k) + F_1w(k), \\ y(k) = C_1x(k) \end{cases}$$

$$\text{Rule}^2: \quad \text{If } x_2(k) \text{ is } 0, \text{ then}$$
$$\begin{cases} Ex(k+1) = A_2x(k) + B_2\tilde{u}(k) + F_2w(k), \\ y(k) = C_2x(k) \end{cases}$$

where

$$E = \begin{bmatrix} 1 & 0 \\ 0 & 0 \end{bmatrix}, A_1 = \begin{bmatrix} 0.9789 & 7.9192 \\ 0.2 & 1.8 \end{bmatrix}, A_2 = \begin{bmatrix} 0.9789 & 7.9192 \\ 0.2 & 1.92 \end{bmatrix}$$
$$B_1 = B_2 = \begin{bmatrix} 0 \\ -0.1 \end{bmatrix}, F_1 = F_2 = \begin{bmatrix} 0.06 \\ 0.05 \end{bmatrix}, C_1 = C_2 = \begin{bmatrix} 0.1 & 1 \end{bmatrix}$$

Setting the initial condition $x(0) = \hat{x}(0) = [0\ 0]^T$, the data dropouts probabilities as $\theta = 0.2$, the actuator fault parameter was chosen as $\eta = 0.5$, and we specified the desired $L_2 - L_\infty$ performance index $\gamma = 2$. Next, solving the LMIs given in (33) and (34) yielded the gain matrices for both the controller and the observer

$$\begin{aligned} K_p &= \begin{bmatrix} 62.0918 & 798.9586 \end{bmatrix}, K_d = \begin{bmatrix} -266.5782 & -6.1904 \end{bmatrix} \\ L_p &= \begin{bmatrix} -0.2976 & -3.1448 \end{bmatrix}^T, L_d = 10^3 \times \begin{bmatrix} 7.7160 & 77.685 \end{bmatrix}^T \end{aligned} \tag{48}$$

The simulation results from Figures 9–13 fully verify the effectiveness of the proposed control method for DC motor systems. Figures 9 and 10 show the responses of system

states $x_1(k)$ and $x_2(k)$ as well as their observer estimates under 20% data dropout, 50% actuator faults, and their simultaneous occurrence. It can be observed that the estimated states closely track the actual states and converge well under all conditions, which demonstrates the effectiveness and robustness of the proposed observer-based PD control scheme. Figure 11 confirms that the designed observer can accurately reconstruct the system output to provide reliable information for control. Figure 12 illustrates that the control input remains bounded without undesirable chattering. To further verify the $L_2 - L_\infty$ performance, the ratio of $\sqrt{y^T(k)y(k)/\sum_{k=0}^{\infty} w^T(k)w(k)}$ is shown in Figure 13. It is shown that the maximum value of the ratio is 0.0165, which is far below the prescribed bound $\gamma = 2$. Therefore, the simulation outcomes validate that the proposed observer-based PD controller can guarantee stochastic stability while achieving the required $L_2 - L_\infty$ performance level.

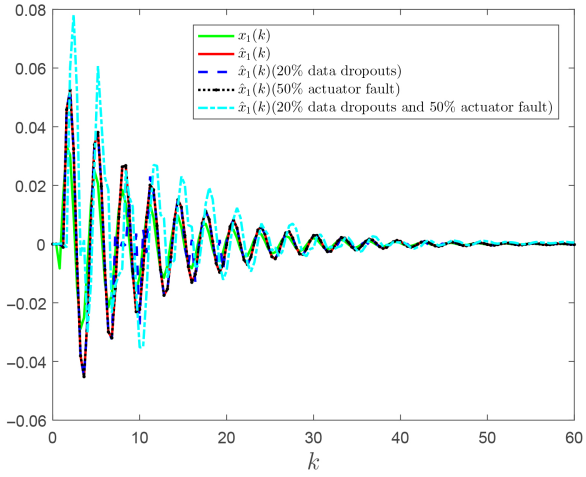


Figure 9. The responses of system state $x_1(k)$ and observer state $\hat{x}_1(k)$ under data dropouts and actuator faults.

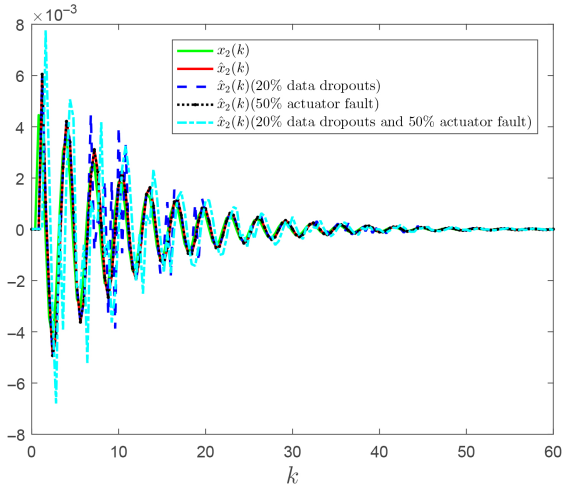


Figure 10. The responses of system state $x_2(k)$ and observer state $\hat{x}_2(k)$ under data dropouts and actuator faults.

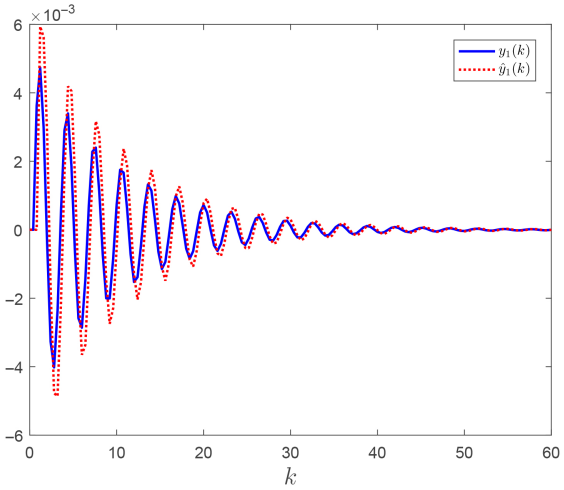


Figure 11. The responses of system output $y(k)$ and observer output $\hat{y}(k)$.

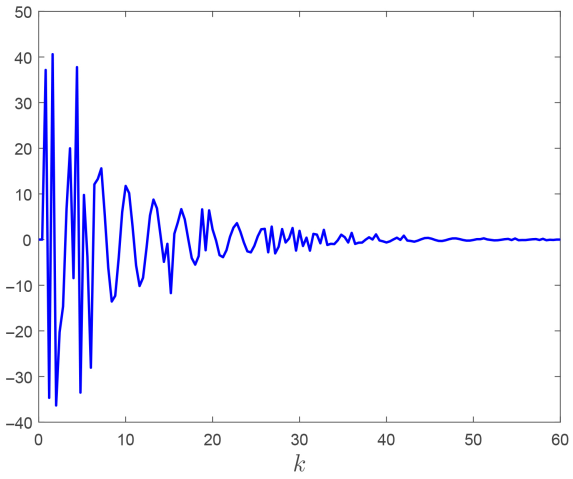


Figure 12. The responses of control input $u(k)$.

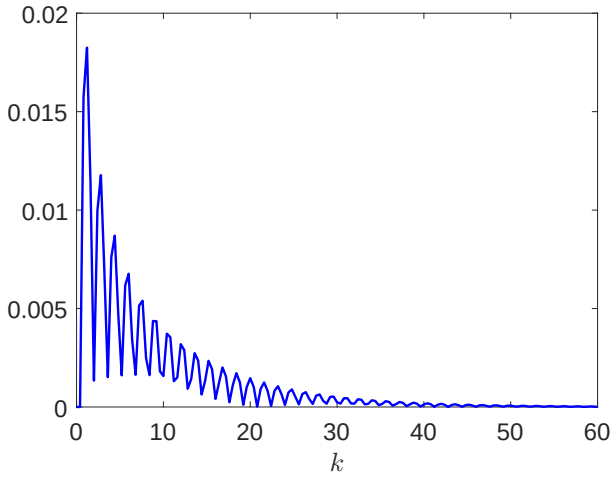


Figure 13. Ratio of $\sqrt{y^T(k)y(k)/\sum_{k=0}^{\infty} w^T(k)w(k)}$.

5. Conclusions

This paper investigated the observer-based PD control strategies for discrete-time descriptor systems subject to network-induced data dropouts and actuator faults. By integrating the T-S fuzzy modeling approach with a generalized descriptor representation,

a unified and tractable control design approach was developed to address the intrinsic challenges arising from system singularity and stochastic disturbances. An observer-based PD control architecture was proposed, in which the derivative component was incorporated into both the controller and the observer structures. This design effectively alleviated the restrictive structural constraints imposed by the singular system matrix and avoided the explicit treatment of regularity and causality conditions. As a result, the analytical complexity of the controller synthesis procedure was significantly reduced. Sufficient conditions guaranteeing stochastic stability and a prescribed $L_2 - L_\infty$ performance level were derived in terms of LMIs, enabling the simultaneous computation of the controller and observer gains via convex optimization techniques. The performance of the proposed methodology was thoroughly evaluated through extensive numerical simulations conducted on a biological economic system and a DC motor driving model, demonstrating superior disturbance rejection and fault tolerance. Future research directions may include extending the developed framework to more general networked control scenarios, such as systems with quantization [45], multiple packet dropout channels [46,47], or deception attacks. In addition, the integration of event-triggered mechanisms and distributed control architectures for large-scale singular systems represents a promising avenue for further investigation.

Author Contributions: Conceptualization, Q.Y.; software, Q.Y. and M.-Y.Q.; validation, Q.Y.; writing—original draft preparation, Q.Y.; writing—review and editing, Q.Y. and X.-H.C. All authors have read and agreed to the published version of the manuscript.

Funding: This work was supported by the National Natural Science Foundation of China under Grant 61773298 and Grant 62173261.

Institutional Review Board Statement: Not applicable.

Informed Consent Statement: Not applicable.

Data Availability Statement: Data are contained within the article.

Conflicts of Interest: The authors declare no conflicts of interest.

References

1. Kchaou, M.; Regaieg, M.A.; Jerbi, H. Admissible control for non-linear singular systems subject to time-varying delay and actuator saturation: An interval type-2 fuzzy approach. *Actuators* **2023**, *12*, 30. [CrossRef]
2. Ku, C.-C.; Chang, W.-J.; Huang, Y.-M. Robust observer-based fuzzy control via proportional derivative feedback method for singular Takagi–Sugeno fuzzy systems. *Int. J. Fuzzy Syst.* **2022**, *24*, 3349–3365. [CrossRef]
3. Yang, Q.; Chang, X.-H. Energy-to-Peak Controller Design for Discrete-Time Singular System. *Circuits Syst. Signal Process.* **2023**, *42*, 5944–5957. [CrossRef]
4. Qiao, M.; Chang, X.-H. Quantified guaranteed cost fault-tolerant control for continuous-time fuzzy singular systems with sensor and actuator faults. *IEEE Trans. Fuzzy Syst.* **2024**, *32*, 660–670. [CrossRef]
5. Xu, S.; Lam, L. Robust stability and stabilization of discrete singular systems: An equivalent characterization. *IEEE Trans. Autom. Control* **2004**, *49*, 568–574. [CrossRef]
6. Kwon, N.K.; Park, I.S.; Park, P.; Park, C.P. Dynamic output-feedback control for singular Markovian jump system: LMI approach. *IEEE Trans. Autom. Control* **2017**, *62*, 5396–5400. [CrossRef]
7. Sun, Y.; Ma, S. Observer-based finite-time stabilization for discrete-time switched singular systems with quadratically inner-bounded nonlinearities. *Int. J. Robust Nonlinear Control* **2019**, *29*, 2041–2062. [CrossRef]
8. Wang, J.; Ma, S.; Zhang, C.; Fu, M. Finite-time filtering for nonlinear singular systems with nonhomogeneous Markov jumps. *IEEE Trans. Cybern.* **2019**, *49*, 2133–2144. [CrossRef]
9. Chen, J.; Lin, C.; Chen, B. Mixed H_∞ and passive control for singular systems with time delay via static output feedback. *Appl. Math. Comput.* **2017**, *293*, 244–253. [CrossRef]
10. Kang, D.; Park, C. Static output feedback H_∞ control for discrete-time singular systems with structure constraints. *Int. J. Control Autom. Syst.* **2025**, *23*, 600–610. [CrossRef]

11. Chang, X.-H.; Han, X. Observer-based fuzzy $l_2 - l_\infty$ control for discrete-time nonlinear systems. *IEEE Trans. Fuzzy Syst.* **2024**, *32*, 2523–2528. [CrossRef]
12. Chang, W.-J.; Huang, Y.-M.; Lin, Y.-H. Observer-based fuzzy control design for uncertain nonlinear singular systems under multi-performance requirements. *Mathematics* **2023**, *11*, 2632. [CrossRef]
13. Feng, Y.; Yagoubi, M.; Chevrel, P. Extended dissipative control for discrete-time singular systems via dynamic output feedback. *Int. J. Robust Nonlinear Control* **2020**, *30*, 7561–7585.
14. Kchaou, M.; Jerbi, H.; Ali, N.B. H_∞ reliable dynamic output-feedback controller design for discrete-time singular systems with sensor saturation. *Actuators* **2021**, *10*, 196. [CrossRef]
15. Ren, J.; Zhang, Q. Non-fragile PD state H_∞ control for a class of uncertain descriptor systems. *Appl. Math. Comput.* **2012**, *218*, 8806–8815. [CrossRef]
16. Zhang, G.; Liu, W. Impulsive mode elimination for descriptor systems by a structured P-D feedback. *IEEE Trans. Autom. Control* **2011**, *56*, 2968–2973. [CrossRef]
17. Duan, G.; Zhang, B. Robust control system design using proportional plus partial derivative state feedback. *Acta Autom. Sin.* **2007**, *33*, 506–510. [CrossRef]
18. Feng, Z.; Zhang, H. State and static output feedback control of singular Takagi-Sugeno fuzzy systems with time-varying delay via proportional plus derivative feedback. *Inf. Sci.* **2022**, *608*, 1334–1351. [CrossRef]
19. Ku, C.; Chang, W. Observer-based proportional derivative fuzzy control for singular Takagi-Sugeno fuzzy systems. *Inf. Sci.* **2021**, *570*, 815–830. [CrossRef]
20. Takagi, T.; Sugeno, M. Fuzzy identification of systems and its applications to modeling and control. *IEEE Trans. Syst. Man Cybern.* **1985**, *15*, 116–132. [CrossRef]
21. Cao, J.-N.; Chen, H. Mathematical model for fault handling of singular nonlinear time-varying delay systems based on T-S fuzzy model. *Mathematics* **2023**, *11*, 2547. [CrossRef]
22. Sun, X.; Zhang, Q. Observer-based adaptive sliding mode control for T-S fuzzy singular systems. *IEEE Trans. Syst. Man Cybern.* **2018**, *50*, 4438–4446. [CrossRef]
23. Feng, Z.; Zhang, H. New results on dissipative control for a class of singular Takagi-Sugeno fuzzy systems with time delay. *IEEE Trans. Fuzzy Syst.* **2022**, *30*, 2466–2475. [CrossRef]
24. Mu, Y.; Zhang, H.; Sun, S. Robust non-fragile proportional plus derivative state feedback control for a class of uncertain Takagi-Sugeno fuzzy singular systems. *J. Frankl. Inst.* **2019**, *356*, 6208–6225. [CrossRef]
25. Chang, W.; Lian, K.; Su, C. Multi-constrained fuzzy control for perturbed T-S fuzzy singular systems by proportional-plus-derivative state feedback method. *Int. J. Fuzzy Syst.* **2021**, *23*, 1972–1985. [CrossRef]
26. Zhang, X.; Jin, K. Proportional plus derivative state feedback control of Takagi-Sugeno fuzzy singular fractional order systems. *Intell. Control Appl.* **2021**, *19*, 3823–3829. [CrossRef]
27. Zhang, L.; Gao, H.; Kaynak, O. Network-induced constraints in networked control systems—A survey. *IEEE Trans. Ind. Inform.* **2013**, *9*, 403–416. [CrossRef]
28. Ma, S.; Boukas, E.K. Stability analysis and H_∞ control for singular networked control systems with packet dropouts. *Automatica* **2012**, *48*, 915–920.
29. Zhang, X.; Han, Q.; Ge, X. Quantized H_∞ control for networked control systems with packet dropouts. *IEEE Trans. Syst. Man Cybern. Syst.* **2020**, *50*, 1529–1539.
30. Zhang, L.; Gao, H. Network-induced constraints in discrete-time systems: Packet loss modeling. *IEEE Trans. Cybern.* **2016**, *46*, 1482–1493.
31. Zhang, H.; Feng, G.; Yan, H. Observer-based H_∞ control for fuzzy networked systems with packet dropouts under the scheduling of Round-Robin protocol. *IEEE Trans. Cybern.* **2019**, *49*, 2205–2216.
32. Chang, X.-H.; Liu, Y. Robust H_∞ filtering for vehicle sideslip angle with quantization and date dropouts. *IEEE Trans. Veh. Technol.* **2020**, *69*, 10435–10445. [CrossRef]
33. Schenato, L.; Sinopoli, B.; Franceschetti, M.; Poolla, K.; Sastry, S.S. Foundations of control and estimation over lossy networks. *Proc. IEEE* **2007**, *95*, 163–187. [CrossRef]
34. Shi, Y.; Yu, B. Output feedback stabilization of networked control systems with random delays modeled by Markov chains. *IEEE Trans. Autom. Control* **2009**, *54*, 1668–1674.
35. Lian, J.; Zhang, C.; Shi, P. Robust H_∞ control for switched systems with time-varying delays and packet dropouts. *Appl. Math. Comput.* **2011**, *217*, 9509–9518.
36. Zhai, G.; Hu, B.; Yasuda, K.; Michel, A.N. Stability analysis of switched systems with stable and unstable subsystems: An average dwell time approach. *Int. J. Syst. Sci.* **2001**, *32*, 1055–1066. [CrossRef]
37. Guo, Z.; Niu, Y.; Wang, H. Fault tolerant control for switched nonlinear systems with packet dropouts and actuator faults. *Appl. Math. Comput.* **2014**, *240*, 109–120.

38. Shi, H.; Yang, C. Robust predictive fault-tolerant control based on signal compensation for nonlinear industrial processes with partial actuator failures. *Int. J. Control* **2026**. [CrossRef]
39. Wang, J.; Zheng, Y.; Ding, J. Memory-based event-triggered fault-tolerant consensus control of nonlinear multi-agent systems and its applications. *IEEE Trans. Autom. Sci. Eng.* **2024**, *22*, 7941–7954. [CrossRef]
40. Kchaou, M.; Souissi, M.; Toumi, A. Delay-dependent stability and robust $L_2 - L_\infty$ control for a class of fuzzy descriptor systems with time-varying delay. *Int. J. Robust Nonlinear Control* **2013**, *23*, 284–304. [CrossRef]
41. Du, H.; Lam, J. Energy-to-peak performance controller design for building via static output feedback under consideration of actuator saturation. *Comput. Struct.* **2006**, *84*, 2277–2290. [CrossRef]
42. Gao, Z.; Wang, Z.; Ji, Z.; Liu, Y. Output strictly passive H_∞ control of discrete-time linear switched singular systems via proportional plus derivative state feedback. *Circuits Syst. Signal Process.* **2020**, *39*, 3907–3924. [CrossRef]
43. Chang, W.; Tsai, M. Observer-based fuzzy controller design for nonlinear discrete-time singular systems via proportional derivative feedback scheme. *Appl. Sci.* **2021**, *11*, 2833. [CrossRef]
44. Aslam, M.S. $L_2 - L_\infty$ control for delayed singular markov switch with nonlinear actuator faults. *Int. J. Fuzzy Syst.* **2021**, *23*, 2297–2308. [CrossRef]
45. Chang, X.-H.; Liu, X.-M.; Hou, L.-W.; Qi, J.-H. Quantized fuzzy feedback control for electric vehicle lateral dynamics. *IEEE Trans. Syst. Man Cybern. Syst.* **2024**, *54*, 2331–2341. [CrossRef]
46. Liu, X.-M.; Chang, X.-H. Adaptive event-triggered tracking control for nonlinear networked systems with dynamic quantization and deception attacks. *Int. J. Robust Nonlinear Control* **2024**, *34*, 8311–8333. [CrossRef]
47. Liu, X.-M.; Chang, X.-H.; Hou, L.-W. Attack-dependent adaptive event-triggered security fuzzy control for nonlinear networked cascade control systems under deception attacks. *Mathematics* **2024**, *12*, 3385. [CrossRef]

Disclaimer/Publisher's Note: The statements, opinions and data contained in all publications are solely those of the individual author(s) and contributor(s) and not of MDPI and/or the editor(s). MDPI and/or the editor(s) disclaim responsibility for any injury to people or property resulting from any ideas, methods, instructions or products referred to in the content.